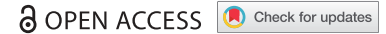









REPORT



NHDL, a recombinant V_L/V_H hybrid antibody control for IgG2/4 antibodies

Corinna Lau ^a, Martin Berner McAdam^b, Grethe Bergseth^a, Algirdas Grevys^{b,c}, Jack Ansgar Bruun ^d, Judith Krey Ludviksen^a, Hilde Fure ^a, Terje Espevik ^e, Anders Moen ^f, Jan Terje Andersen ^{b,g}, and Tom Eirik Mollnes ^{a,e,h,i}

^aResearch Laboratory, Nordland Hospital Trust, Bodø, Norway; ^bDepartment of Immunology, Oslo University Hospital-Rikshospitalet, and Centre for Immune Regulation, Oslo, Norway; ^cCentre for Immune Regulation and Department of Biosciences, University of Oslo, Oslo, Norway; ^dDepartment of Medical Biology, Proteomics Platform, University of Tromsø, Tromsø, Norway; ^eCentre of Molecular Inflammation Research, and Department of Cancer Research and Molecular Medicine, Norwegian University of Science and Technology, Trondheim, Norway; ^fDepartment of Biosciences, Proteomics core facility, University of Oslo, Oslo, Norway; ^gDepartment of Pharmacology, Institute of Clinical Medicine, Oslo University Hospital and University of Oslo, Oslo, Norway; ^hDepartment of Immunology, Oslo University Hospital, University of Oslo, Oslo, Norway; ⁱFaculty of Health Sciences and K. G. Jebsen TREC, University of Tromsø, Tromsø, Norway

ABSTRACT

The mechanism of action of recombinant IgG2/4 antibodies involves blocking of their target without the induction of effector functions. Examples are eculizumab (Soliris[®]), which is used clinically to block complement factor C5, as well as anti-human CD14 (r18D11) and anti-porcine CD14 (rMIL2) produced in our laboratory. So far, no proper IgG2/4 control antibody has been available for controlled validation of IgG2/4 antibody functions. Here, we describe the design of a recombinant control antibody (NHDL), which was generated by combining the variable light (V_L) and heavy (V_H) chains from two unrelated specificities. NHDL was readily expressed and purified as a stable IgG2/4 antibody, and showed no detectable specificity toward any putative antigen present in human or porcine blood. The approach of artificial V_L/V_H combination may be adopted for the design of other recombinant control antibodies.

ARTICLE HISTORY

Received 28 August 2019
Revised 15 October 2019
Accepted 25 October 2019

KEYWORDS

Recombinant antibody;
control antibody; IgG2/4;
hybrid; therapeutic antibody



Introduction

Antibodies are the fastest growing class of biologics, and more than 60 antibody-based drugs have been approved for clinical use.¹ In addition, hundreds of antibodies are undergoing pre-clinical and clinical testing for the treatment of a variety of diseases and disorders, including inflammation and cancer, and novel mechanisms of action and delivery strategies are being explored.¹ These antibodies bind their cognate antigen and induce Fc-mediated effector functions through the engagement of complement or Fc receptors, which may result in antibody-dependent complement-mediated cell lysis, antibody-dependent cellular phagocytosis or antibody-dependent cell-mediated cytotoxicity (ADCC).


Humans have four IgG subclasses (IgG1, 2, 3 and 4) with very distinct abilities to induce effector functions. The subclasses share about 90% similarities in amino acid composition, where minor differences between them affect their ability to engage an antigen and to induce effector functions.² IgG1 and IgG3 are the most efficient triggers of effector functions, and since IgG1 has a longer serum half-life, it is the preferred subclass for the development of therapeutic antibodies.^{2,3} In addition, the composition of the biantennary *N*-glycan structures attached to Asn297 of the C_{H2} domain determines the potency of effector functions through activation of FcγRs and complement C1, and, therefore, glycoengineering can be used to tailor IgG molecules.^{4,5}

When the main aim of a therapeutic antibody is to block the function of the targeted antigen, it may be desirable to design the antibody with reduced ability to induce effector functions, while retaining long serum half-life. This may be achieved, for example, by means of aglycosylated IgG or site-specific mutations.^{5–7} Saunders has written a comprehensive review of this topic.⁸ As IgG2 and IgG4 are the least effector potent subclasses, they can be combined in the design of “effector-less” antibodies, like IgG2m4 and IgG2σ, in which IgG4 key residues have been introduced in the IgG2 Fc backbone by point mutations,^{9,10} or recombinant IgG2/4 C_H hybrid antibodies (in short IgG2/4), where the C_{H1} and hinge region from IgG2 are fused to the C_{H2} and C_{H3} domains from IgG4.^{11–14}

One such IgG2/4 antibody is the anti-human complement factor C5 antibody eculizumab (Soliris[®]), which is approved by the United States Food and Drug Administration (FDA) for treatment of the rare diseases paroxysmal nocturnal hemoglobinuria, atypical hemolytic uremic syndrome and myasthenia gravis. These diseases are all caused by dysregulation of the complement system,^{14–16} which is part of the body's first line of defense. It is activated by both pathogenic and endogenous danger signals, and acts by opsonization, anaphylatoxyn, and signal transduction. Complement activation is tightly controlled and dysregulation may cause rare and common diseases, which in some cases may be life-threatening.^{17–19} Thus, eculizumab

CONTACT Corinna Lau  corinna.lau@nlsh.no  Research Laboratory, Nordland Hospital Trust, Parkveien 95, Bodø 8092, Norway

This article has been republished with minor changes. These changes do not impact the academic content of the article.

 Supplemental data for this article can be accessed on the [publisher's website](#).

© 2019 The Author(s). Published with license by Taylor & Francis Group, LLC.

This is an Open Access article distributed under the terms of the Creative Commons Attribution-NonCommercial License (<http://creativecommons.org/licenses/by-nc/4.0/>), which permits unrestricted non-commercial use, distribution, and reproduction in any medium, provided the original work is properly cited.

and other complement-inhibitory drugs are not only critical for treatment of such diseases, but also important tools for studying them.^{20–23}

Since the IgG2/4 backbone is already used in a marketed product, we constructed two such antibodies in our laboratory for neutralization of human and porcine CD14 in different sepsis models, and reported the results of studies exploring their properties.^{12,24,25} CD14 is a cofactor of several Toll-like receptors (TLRs), including TLR2 and TLR4, that are the second branch of innate immunity against pathogenic and endogenous danger. CD14 facilitates pattern recognition of mainly acylated structural components like Gram-negative bacterial lipopolysaccharide (LPS), and induces the expression of proinflammatory cytokines and type I interferons through TLR signaling.^{26–29} Recently, increased plasma levels of a 13 kDa soluble CD14 subtype (sCD14-ST; presepsin) have emerged as an early sepsis marker.³⁰ Although the blocking of CD14 has been shown to be beneficial in various experimental sepsis models, the strategy has failed in clinical trials. Due to signaling crosstalk between CD14/TLRs and complement, a more potent therapeutic strategy to treat sepsis, however, seems to be the combined inhibition of CD14 and complement, as successfully demonstrated in mice and porcine models.^{25,31,32} This approach may also be effective in the treatment of acute sterile inflammatory conditions like trauma and ischemia-reperfusion injury.^{32,33}

As for any experimental set-up, for studies where IgG2/4 C_H hybrid antibodies are attractive tools, proper controls are needed. Earlier, we designed a putative IgG2/4 control antibody (raNIP) directed toward the hapten hydroxy-3-iodo-5-nitrophenylacetic acid.¹² However, this antibody was expressed at low titers and induced unwanted adverse effects

when applied *ex vivo* in human and porcine whole blood. Here, we aimed to construct a novel IgG2/4 control antibody with improved properties, *i.e.*, high expression level and structural integrity, as well as minimum effector functions and adverse effects.

Results

Construction of NHDL: an IgG2/4 control antibody

We hypothesized that the construction of an IgG2/4 control antibody could be achieved by combining the cDNA encoding the variable light and heavy domains from antibodies of two unrelated specificities. To test this, we took advantage of a panel of previously designed IgG2/4 antibodies, namely r18D11, rMil2, and raNIP, which encode anti-human CD14 (clone 18D11), anti-porcine CD14 (clone Mil2) and anti-NIP (aNIP) specificities, respectively.¹² All possible combinations of two vectors encoding their variable light (V_L) or variable heavy (V_H) regions, upstream of the respective light chain (pLNOK) or heavy chain (pLNOH) constant regions, were transiently transfected into adherent HEK293E cells. Three days post transfection, three of six combinations were shown to yield secreted antibodies (Figure 1a). It appeared that the V_L with anti-human CD14 specificity (clone 18D11) was most suited for V_H/V_L combinations, and yielded expressed antibodies that included any of the tested V_H. Based on this observation, and in order to avoid two anti-CD14 specificities in the same antibody molecule, we chose to proceed with the evaluation of the V_H/V_L hybrid bearing the aNIP V_H and the 18D11 V_L (Figure 1b), named NHDL, as a putative IgG2/4 control antibody.

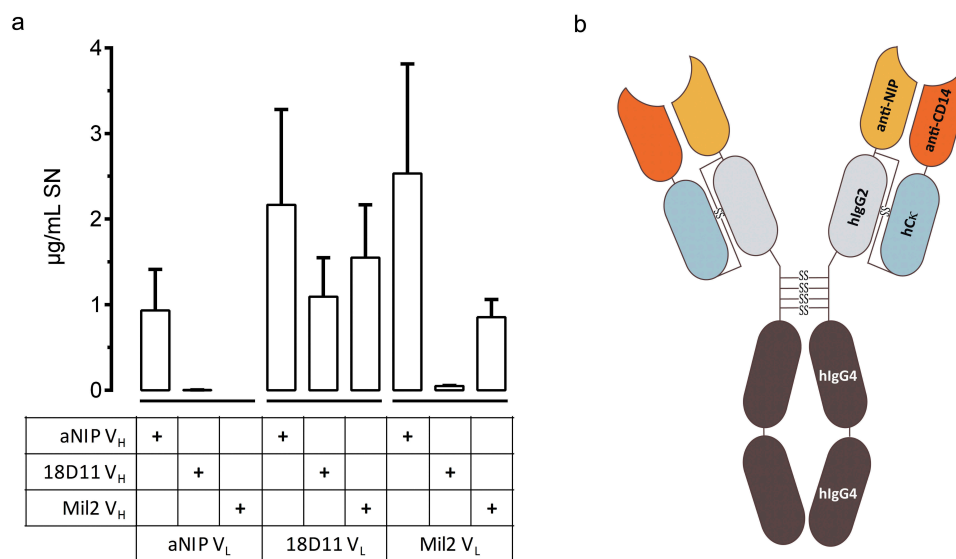


Figure 1. Composition of IgG2/4 control antibody NHDL.

A, The expression of all possible V_L/V_H combinations for IgG2/4 control antibody generation was tested by transient transfection of HEK293E cells with different combinations of the two separate DNA plasmids encoding the light (V_L+C_L; pLNOK) or heavy (V_H+C_H; pLNOH) chains of anti-NIP (aNIP), anti-porcine CD14 (Mil2) or anti-human CD14 (18D11) specificities. Cell culture supernatant (SN) was harvested 3 days post transfection and IgG titer was estimated as µg/mL using ELISA (n = 3; mean ± S.E.M.). B, Schematic model of NHDL, a mouse/human chimeric IgG2/4 antibody. The constant regions, *i.e.*, human kappa light chain (hCκ; blue), human IgG2 C_H1/hinge (light gray) and human IgG4 C_H2-3 (dark gray), are identical for the IgG2/4 C_H hybrid antibodies described so far, *i.e.*, NHDL, r18D11, rMil2, and eculizumab. The murine variable regions of NHDL are derived from two different specificities, *i.e.*, V_H of anti-NIP (yellow) and V_L of anti-CD14 clone 18D11 (orange). The model was generated using Adobe Illustrator.

When NHDL was expressed following a previously established 12-day batch-batch protocol for medium scale production in HEK293E cells,¹² it was produced with a similar profile over time as the other IgG2/4 antibodies (Figure S1a). Further, NHDL ($21.6 \pm 6.2 \mu\text{g}/10^6$ cells) was produced in similar amounts as r18D11 ($30.0 \pm 5.4 \mu\text{g}/10^6$ cells), but in fourfold higher amounts when compared with raNIP ($5.7 \pm 1.1 \mu\text{g}/10^6$ cells) (Figure S1b). Also, NHDL was easily obtained by Protein A-assisted affinity chromatography (Figure S1c), which enabled us to perform a thorough characterization of this putative control antibody.

Structural integrity of NHDL compared to other IgG2/4 antibodies

The structural integrity of NHDL was evaluated by SDS-PAGE, size exclusion chromatography (SEC) and differential scanning fluorimetry (DSF), and compared to other IgG2/4 antibodies, *i.e.*, anti-human C5 (eculizumab), anti-NIP (raNIP), anti-human CD14 (r18D11), and anti-porcine CD14 (rMil2). Non-reducing SDS-PAGE analysis revealed that all IgG2/4 antibodies migrated as one major band corresponding to molecular weights above 150 kDa, which is expected for *N*-glycosylated monomeric IgG (Figure 2a). This was confirmed by SEC, where one main peak was detected for all antibodies (Figure 2b). However, additional peaks were observed for r18D11, rMil2 and raNIP, indicating the presence of non-covalent oligomers (r18D11, rMil2) or higher-

order aggregates (raNIP). In addition, r18D11 eluted somewhat earlier than the other IgG2/4 antibodies, likely due to distinct structural properties of this particular antibody, which can affect retention on the SEC column.

Next, thermal unfolding was measured using DSF where the recombinant IgG2/4 antibodies exerted melting temperatures (T_m) in the range of 68.5°C to 64.9°C , similar to commercial eculizumab, which has a T_m of 68.2°C (Figure 2c). In contrast to NHDL, and any other IgG2/4 antibody, the DSF profile of raNIP showed a high fluorescence background signal below 40°C .

Taken together, the exchange of anti-NIP V_L in raNIP with anti-human CD14 V_L of r18D11, combined with anti-NIP V_H , gave rise to a more efficiently produced and structurally more stable recombinant IgG2/4 molecule, namely NHDL.

NHDL as control for anti-human CD14 r18D11

Next, it was essential to test for the remaining antigen-binding properties of NHDL. This was done by incubating equimolar amounts of recombinant soluble human CD14 (sCD14) with NHDL or anti-CD14 antibody r18D11 before samples were applied to native polyacrylamide gel electrophoresis, which revealed complex formation between sCD14 and r18D11 but not NHDL (Figure 3a). To confirm this *ex vivo*, up to $10 \mu\text{g}/\text{mL}$ R-phycoerythrin (PE)-conjugated NHDL or r18D11 were

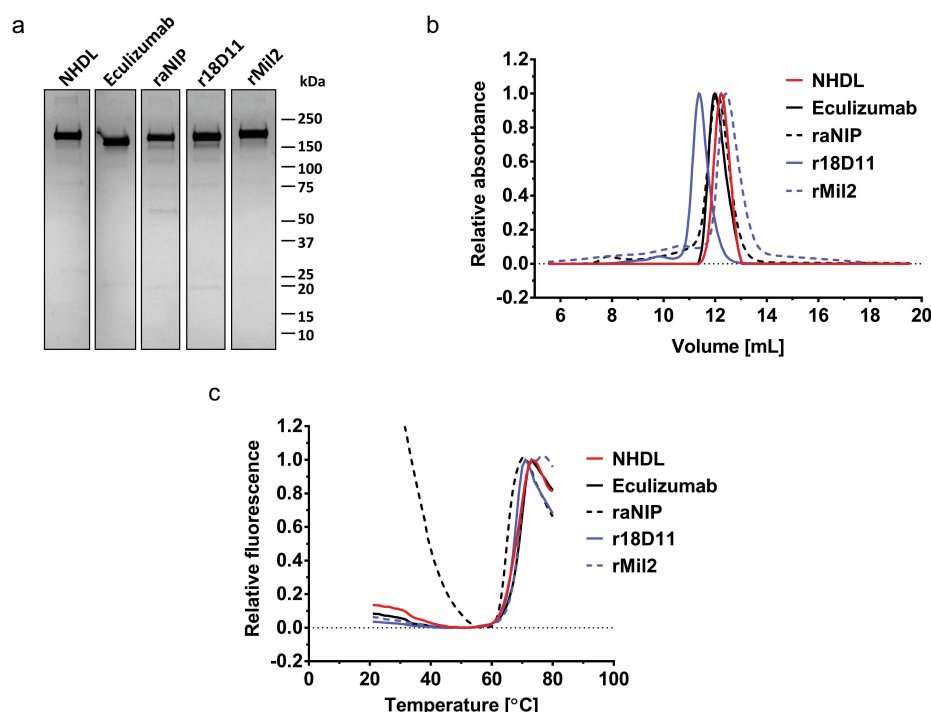


Figure 2. Structural integrity of NHDL compared to other IgG2/4 antibodies.

a, The IgG2/4 antibodies NHDL, raNIP, and r18D11, all purified from the supernatant of transiently expressing HEK293E cells, as well as rMil2 and eculizumab were subjected to non-reducing SDS-PAGE (4–15%) using Precision Plus Protein™ standard as protein ladder. b, Size exclusion chromatography profiles of the indicated IgG2/4 antibodies were normalized to a relative absorbance maximum of 1.0 and displayed as an overlay. Fractions of monomeric single IgG molecules were contained by the main peaks between 11.4 mL and 12.5 mL, while IgG oligomers or aggregates appeared earlier and as minor peaks. Note that r18D11 eluted slightly earlier than the other IgG2/4 antibodies. c, Monomeric IgG2/4 antibody fractions prepared by SEC were subjected to differential scanning fluorimetry and melting curves were generated for temperatures between 20°C to 80°C . Dye incorporation increases as proteins disassemble, reaching a maximum of around 70°C prior to aggregation and decrease of the signal. The derived melting temperatures were 67.7°C for NHDL, 64.9°C for r18D11, 68.5°C for rMil2, and 68.2°C for eculizumab. The melting curve of raNIP showed unusual high background fluorescence below 40°C , in the so-called native state.

incubated with fresh human whole blood, and cell surface binding to human CD14 was monitored using flow cytometry (Figure 3b). While a concentration-dependent increase in fluorescence signals, indicating binding, was detected for r18D11, no such signals were obtained for NHDL. In line with this, when added, unlabeled NHDL did not compete for the binding of the PE-conjugated anti-CD14 antibody (Figure 3b).

In accordance with CD14 being the LPS receptor, binding of r18D11 to CD14 has been shown to block LPS-induced inflammatory cytokine release from responding blood cells.^{12,28} When comparing r18D11 with NHDL *ex vivo* in human whole blood, no effect of NHDL on the CD14-dependent interleukin (IL)-6 release was detected (Figure 3c). Thus, NHDL does not bind or block human CD14 and can be used to control the activity of r18D11.

Blood plasma protein binding by IgG2/4 antibodies

In order to exclude the possibility that NHDL specifically recognized any antigen contained by human blood plasma, we compared the immunoprecipitation of plasma proteins by NHDL with that by r18D11, and eculizumab. The antibodies were coupled to magnetic beads, followed by incubation with human plasma and a washing procedure. Immunoprecipitated

proteins were subjected to mass spectrometry and a sequence database search. In total, 66 proteins, including immunoglobulins and transport proteins, were shown to potentially bind at least one of the antibodies, including a bead-coupled control IgG with irrelevant specificity (anti-human CD3 mouse IgG1). Cluster analyses revealed that the immunoprecipitation profiles for the IgG2/4 antibodies were rather similar (Figure S2a). Only 14 of the identified proteins were non-IgG sequences with peptide-spectrum match scores (#PSM; a signal quality measure) above 10 and higher for NHDL than for the control IgG. Spectrum peak area intensities of the peptides contained by the immunoprecipitated proteins were used to quantitatively compare potential binding by NHDL, r18D11 and eculizumab (Figure 3d). As expected, among the proteins that were immunoprecipitated by eculizumab and r18D11, their cognate antigens human C5 and CD14, respectively, were identified with the highest intensities. Importantly, for NHDL, none of the identified proteins, including CD14 and C5, were immunoprecipitated from human plasma with a considerably higher score than for the other IgG2/4 antibodies (Figure 3d). This indicates that human plasma does not contain any putative antigen for NHDL.

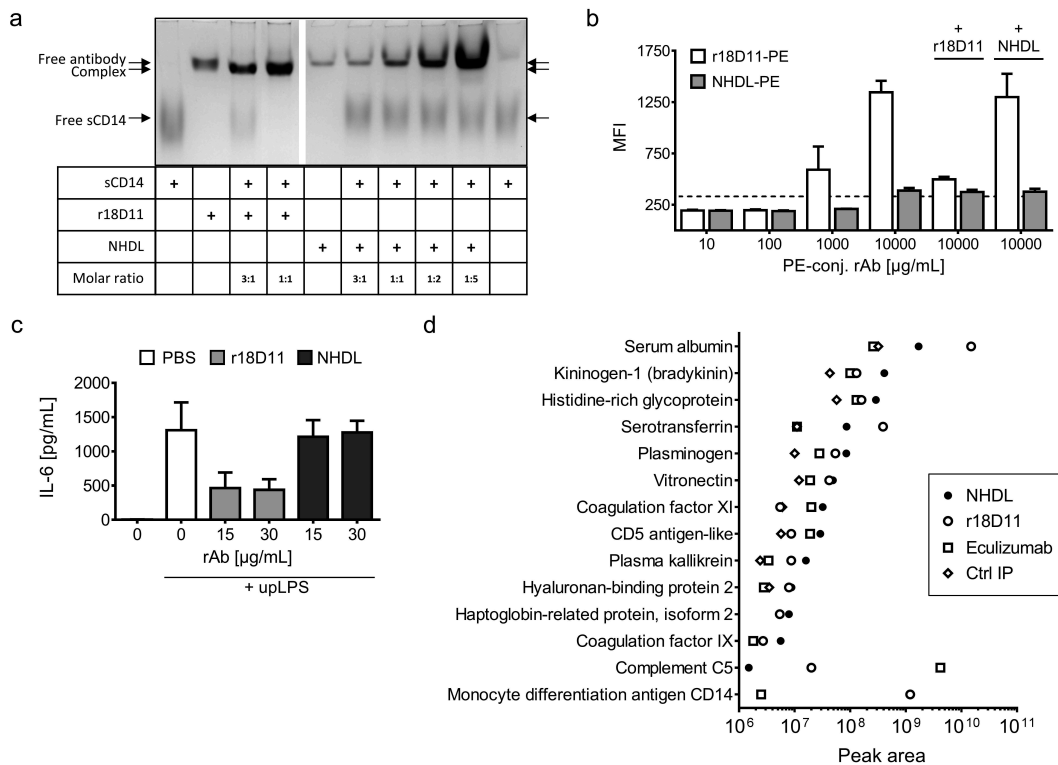


Figure 3. Test of binding and blocking activity of human CD14 by NHDL.

a, Different molar ratios of purified antibody (r18D11 or NHDL) and recombinant soluble CD14 (sCD14) (given as antigen to antibody) were incubated *in vitro* and subsequently separated by native PAGE in absence of SDS. The antigen-antibody complex formation became apparent as a newly formed band and a reduction in or loss of the bands corresponding to free antibody or free sCD14. All three bands are indicated by arrows. b, Human whole blood was incubated with 10–10,000 ng/mL of PE-conjugated NHDL or r18D11. Binding was analyzed by flow cytometry and given as mean fluorescence intensity (MFI). For competitive binding, blood was pre-incubated with 15 μg/mL unconjugated r18D11 or NHDL prior to the addition of the PE-conjugated antibodies. Results are shown as MFI (n = 3; mean ± S.E.M.). The MFI (330 ± 9.8) of a PE-conjugated mIgG1 control antibody is indicated by the dotted line. c, Whole human blood was incubated with PBS or 100 ng/mL upLPS in absence or presence of 15 μg/mL or 30 μg/mL r18D11 or NHDL for 120 min at 37°C. Plasma IL-6 levels were analyzed by Bioplex technology and are given in pg/mL (n = 3; mean ± S.E.M.). d, human plasma (a pool of n = 6) was incubated with Dynabeads[®]-coupled NHDL, r18D11, eculizumab, or a control antibody (Ctrl IP; anti-CD3 mIgG1), and co-immunoprecipitated proteins were identified using mass spectrometry. The results are shown for non-IgG sequences with #PSM > 10 and peak area values larger for NHDL than for the control antibody (Ctrl IP). The unfiltered results are displayed as a heatmap in Figure S2a.

NHDL as control for anti-human C5 eculizumab and anti-porcine CD14 rMil2

Next, we addressed whether NHDL could be used as a control antibody for the IgG2/4 antibodies eculizumab and rMil2. Using an ELISA established to quantify binding of eculizumab to human C5 in human serum or plasma,³⁴ we confirmed the immunoprecipitation data showing that NHDL did not bind C5 (Figure 4a). To test for C5 inhibition, human plasma was incubated with heat-aggregated IgG (HAiGg) in the presence or absence of NHDL and eculizumab, followed by measuring C5-dependent formation of the soluble terminal complement sC5b-9 complex (TCC) (Figure 4b). In contrast to eculizumab, TCC generation was not abolished in the presence of NHDL. Thus, NHDL proved inert with respect to both C5 binding and blocking.

To compare NHDL with rMil2 in porcine CD14 binding and inhibition, fresh porcine blood was drawn and subjected to flow cytometry and immunoprecipitation-tandem mass spectrometry (MS/MS) for binding assays, as well as to the *ex vivo* whole blood model (Figure 4c and S3). In flow cytometry, neither binding of NHDL to porcine white blood cells (Figure S3a) nor competition of the positive signal for fluorescein isothiocyanate (FITC)-conjugated Mil2 binding to porcine CD14 positive blood cells were detected (Figure 4c). Also, binding of NHDL to porcine blood plasma proteins was tested by immunoprecipitation followed by MS/MS (Figure S3b). Here, no putative antigen could be identified for NHDL, whereas rMil2 readily co-immunoprecipitated with its antigen, porcine CD14.

Further, opposed to rMil2, NHDL did not reduce the *Escherichia coli* (*E. coli*)-induced, partially CD14-dependent

IL-8 release in porcine whole blood (Figure 4d), but rather increased the response somewhat, which is addressed below. Together, NHDL did not bind porcine CD14 and did not block its effects in whole blood.

Nip-binding by NHDL

As NHDL contains a V_H, which is specific for the synthetic hapten NIP, potential binding was tested using ELISA, where bovine serum albumin (BSA)-conjugated NIP was immobilized in a microtiter plate and incubated with up to 10 µg/mL NHDL. In contrast to anti-NIP mIgG1, no binding of NHDL was detected (Figure S4).

NHDL production from stably transfected CHO-K1SP cells

Since NHDL proved suitable as an IgG2/4 control antibody, we aimed to establish a protocol for large-scale production by stably transfected Chinese ovary hamster (CHO)-K1SP cells. Compared to transient expression in HEK293E cells, expression titers were increased by 500 to 1000-fold, yielding 13 mg NHDL and 28 mg r18D11 per 10⁶ CHO-K1SP cells (Figure 5a), or ≥1 mg IgG2/4 antibody per mL supernatant, within 14 days of cultivation.

Expression system-dependent IgG N-glycosylation profiles

The expression system used for recombinant IgG production may affect antibody properties due to differential

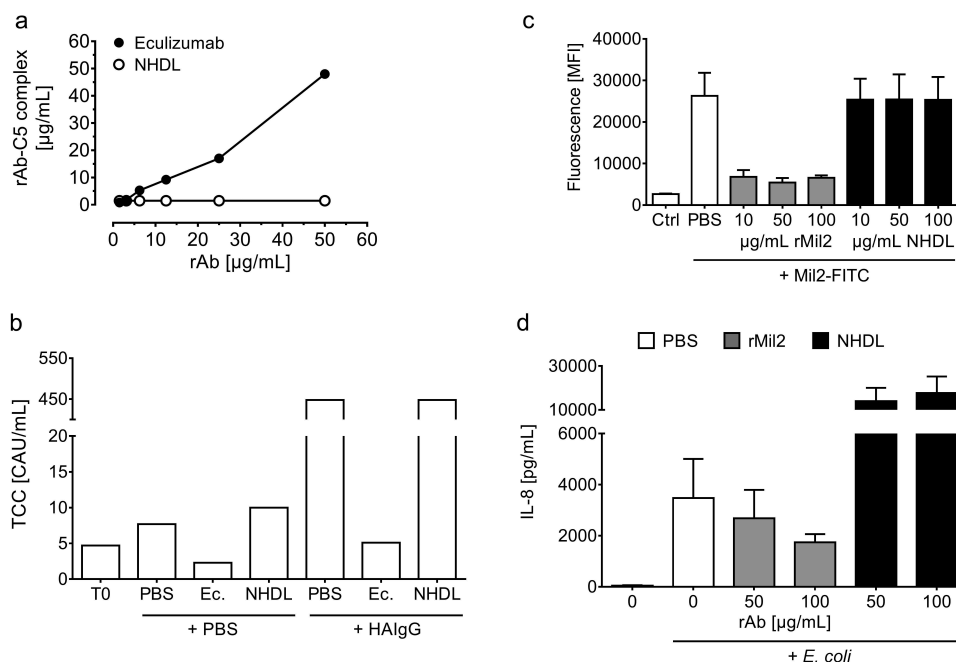


Figure 4. Test of binding and blocking of human C5 and porcine CD14 by NHDL.

a, Increasing amounts (2.5–50 µg/mL) of recombinant antibody (rAb), *i.e.*, NHDL or eculizumab, were incubated with a human serum pool that naturally contains C5, and C5-bound antibody (rAb-C5 complex) was quantified as µg/mL by ELISA according to a standard curve using eculizumab. b, Complement activation in a human serum pool in the presence or absence of 1 mg/mL heat-aggregated IgG (HAiGg) and 200 µg/mL NHDL or eculizumab (Ec.) was measured as TCC formation using ELISA. Data are given as complement arbitrary units (CAU/mL) for one representative experiment. c, Competitive binding of FITC-conjugated Mil2 to porcine whole blood cells in presence of 10, 50 or 100 µg/mL NHDL or rMil2 was measured by flow cytometry. A FITC-conjugated mIgG2b antibody served as a negative control (Ctrl). Results are shown as MFI ($n = 3$; mean \pm S.E.M.). d, *E. coli*-induced (1×10^5 /mL) porcine plasma IL-8 release was measured in the absence or presence of 50 or 100 µg/mL NHDL or rMil2 using Bioplex technology. The results are given as pg/mL ($n = 3$; mean \pm S.E.M.).

N-glycosylation (for reviews, see refs. 4, 34, 35).^{4,35,36} Therefore, *N*-glycosylation profiles of the CHO- and HEK293E-produced IgG2/4 antibodies were mapped using LC-MS (Table S1 and Figure S5). Cell-type specific differences were revealed regarding the degree of terminal galactosidation of 4-*N*-acetylglucosamine-1-fucose-3-mannose (4GlcNAc-1Fuc-3Man), the core structure (G0) of typical Asn297-attached *N*-glycans (Table S1). Despite being the major *N*-glycan attached in all preparations, non-galactosidated G0 constituted a much higher portion of all detected *N*-glycans for NHDL and r18D11 derived from CHO cells compared to those from HEK293E cells (*i.e.*, 79.1% and 75.3% compared to 54.4% and 49.0%, respectively). Notably, differences in the *N*-glycosylation profiles for different IgG2/4 antibodies produced from the same cell line were only minor (Table S1).

Expression system-dependent IgG structural integrity

No difference in IgG integrity could be observed between NHDL and r18D11 derived from CHO cells compared to HEK293E cells, as they migrated with similar bands in non-reducing SDS-PAGE (Figure S6A) and gave very similar melting curves in DSF analyses (Figure S6b and c).

Binding of IgG2/4 antibodies to effector molecules

To address whether the differences in the *N*-glycan profiles affected the binding of the IgG2/4 antibodies to effector molecules, we performed ELISA where titrated amounts of the antibodies were coated followed by the addition of selected human Fcγ receptors or C1q. The results revealed that CHO-produced NHDL and r18D11 did not bind human FcγRI, FcγRIIIa, and C1q, while modest binding to human FcγRIIIa was observed (Figure 5b). In contrast, HEK293E-produced NHDL bound human FcγRI weakly, while HEK293E-produced r18D11 did not (Figure 5b), which is in line with previous observations for HEK293E-produced r18D11.¹² In addition, no major differences in pH-dependent binding to the human and porcine versions of neonatal Fc receptor (FcRn) were detected between the recombinant IgG2/4 antibodies produced from CHO and HEK293E cells (Figure S7).

Inflammatory responses to the IgG2/4 antibodies

Next, we ruled out an influence of the choice of host cell line on the CD14-blocking effect of r18D11 in human whole blood challenged with 100 ng/mL upLPS, while proving that both CHO- and HEK293E-produced NHDL were inactive (Figure 5c). However,

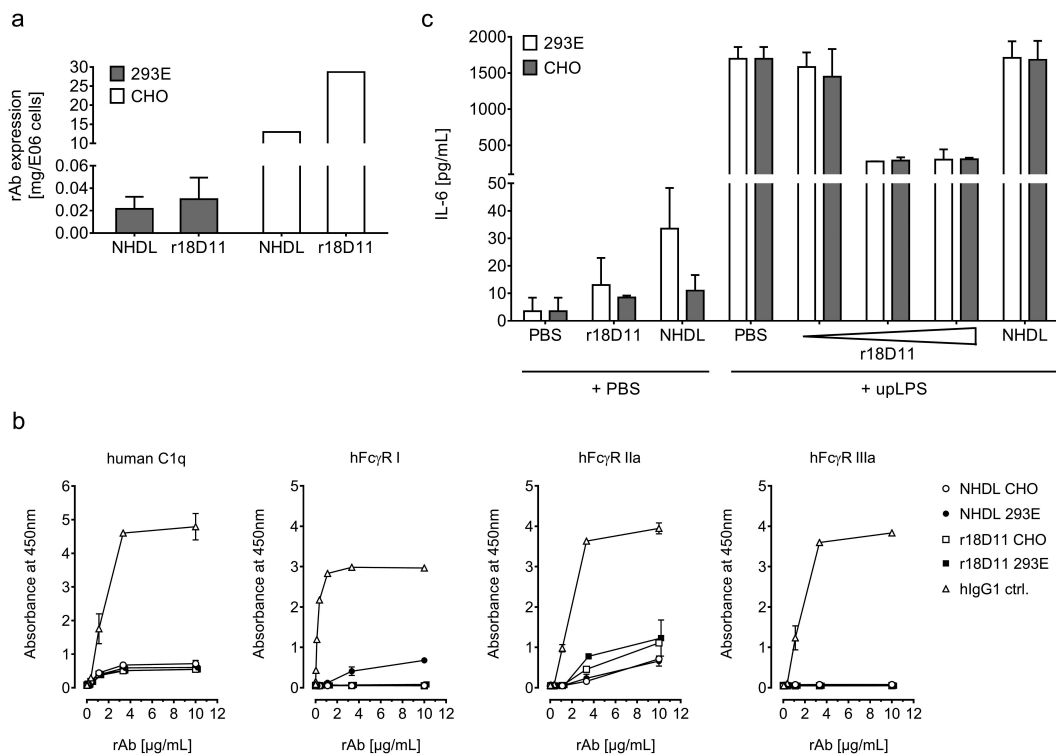


Figure 5. Characterization of CHO-produced NHDL and r18D11.

A, The expression of recombinant NHDL and r18D11 by stably transfected CHO-K1SP cell pools (fed-batch) was compared to transient expression by HEK293E cells (batch-batch). Cell culture supernatants were analyzed for IgG levels using ELISA. Results are given as single value mg IgG per E06 CHO cells ($n = 1$), and mean mg IgG \pm S.E.M. per E06 HEK293E cells for NHDL ($n = 3$) and r18D11 ($n = 6$). B, Binding of increasing concentrations of CHO- and HEK293E-produced NHDL or r18D11 to recombinant human C1q or recombinant human Fcγ receptors hFcγRI, hFcγRIIa, and hFcγRIIIa at pH 7.4 was measured by ELISA. As a positive control, a recombinant human IgG1 antibody (bevacizumab (Avastin®), Roche) was included in the analysis. The results are shown as relative units for the absorbance at 450 nm ($n = 2$; mean \pm S.D.). C, Human whole blood was incubated with CHO- or HEK293E-produced r18D11 (1.5, 15 and 30 μ g/mL) or NHDL (15 μ g/mL) in the presence of 100 ng/mL upLPS. As controls, 15 μ g/mL r18D11 or NHDL were incubated in the presence of PBS, only. Plasma IL-6 was measured using Bioplex technology. Data are given as pg/mL ($n = 2$; mean \pm S.D.).

in the same experiment, we observed that HEK293E-produced NHDL, and to a lesser extent r18D11, induced IL-6 release in absence of upLPS, while CHO-produced NHDL did not to the same extent (Figure 5c). Earlier, we had observed an increased IL-8 release in *E. coli*-challenged porcine blood in the presence of HEK293E-produced NHDL (Figure 4d). This prompted us to evaluate putative cytokine release and complement activation induced by CHO-produced IgG2/4 antibodies when added to whole human or porcine blood (Figure 5c and S8). Indeed, there was minor induction of IL-6 and TCC in human blood (Figure 5c and S8A) and of any tested cytokine and TCC in porcine blood (Figures S8B and S8C). However, these effects were similar for all IgG2/4 antibodies, including commercial eculizumab.

Taken together, NHDL was produced in CHO cells at high titers, with unaffected thermal stabilities and only minor effector functions, which were comparable to other IgG2/4 antibodies, including eculizumab. Therefore, NHDL should be a suitable IgG2/4 control antibody for *ex vivo* testing in human and porcine whole blood as well as in *in vivo* porcine models.

Discussion

Here, we presented a novel IgG2/4 control antibody, called NHDL, which carries the variable regions of two different specificities, and exerts no antigen-binding capacity. Therefore, it can be applied as a negative control for antibodies with the same IgG2/4 C_H hybrid backbone in *in vitro* assays.

The antigen-binding domain of NHDL was designed as an artificial V_L/V_H hybrid, containing the V_L of the human CD14-specific antibody clone 18D11 and the V_H of a synthetic hapten-specific antibody (anti-NIP).¹² Here, we showed that their combination destroyed both specificities, which was a prerequisite for NHDL being suitable as a control antibody. Antibody variable regions are important determinants not only of antigen specificity but also of structural integrity.^{37–40} Our study demonstrated that artificial V_L/V_H combinations can result in readily expressed, properly assembled antibody molecules with structural integrity, as NHDL was expressed as a stable, monomeric IgG2/4 antibody.

NHDL was more inert with respect to the induction of effector functions than the previously described control antibody raNIP.¹² In raNIP, the V_L and V_H regions are identical in amino acid sequence, and one may speculate whether this led to the formation of aggregates and low expression titers.¹² However, raNIP is only unstable in the IgG2/4 kappa background, while the same pairing of variable sequences is readily expressed as recombinant human IgG1 kappa and IgG3 lambda antibodies using the same HEK293E cell-based expression system.^{41,42} Therefore, it remains to be seen whether artificial V_L/V_H combinations may result in properly folded antibodies of any human IgG subclass or format, as well as IgGs from different species.

Further, the generation of artificial non-antigen-binding IgG based on V_L/V_H combination may appear straightforward and cost-efficient when separate heavy and light chain-encoding plasmids for the production of monospecific antibodies are readily available, as was the case with this study.

Although this strategy has limitations, the scientific community has accumulated extensive knowledge about antigen-antibody binding and produced a wide array of engineered antibodies,^{43,44} which may provide alternative routes to generate non-binding control antibodies. However, as antigen-binding capacity can affect an antibody's pharmacokinetic properties,⁴⁵ differences in clearance and tissue distribution of non-binding control antibodies compared to the binding IgG may occur *in vivo*, regardless of the design strategy.

The combination of human IgG2- and IgG4-derived sequences in one hybrid backbone is ingeniously suited when effector functions are to be avoided, since it has very low potential to activate complement and Fcγ receptors.^{9,10,12–14} As elegantly summarized by Saunders, substantial research has been performed on how to minimize effector functions by specific amino acid mutations of human IgG antibodies, and various promising IgG2 and IgG4 variants have been generated.⁸ To our knowledge, three antibodies with the particular IgG2/4 C_H hybrid backbone consisting of IgG2 C_H1/hinge and IgG4 C_H2/C_H3 have been reported, *i.e.*, the US FDA-approved anti-human C5 antibody eculizumab, anti-human CD14 antibody r18D11, and anti-porcine CD14 antibody rMil2.^{12,15,20} NHDL proved to be inert with respect to binding and blocking these antigens *ex vivo* in human and porcine whole blood, as well as to nonspecific binding to any potential antigen contained by human or porcine blood. As such, NHDL is a proper control for epitope neutralization and effector functions of IgG2/4 C_H hybrid antibodies, at least in human and pig disease models.

Importantly, C5 and CD14 are upstream inflammatory mediators, and inhibition of these, either alone or in combination, has substantial potential in various diseases.⁴⁶ Eculizumab has been approved for the treatment of three complement-dependent diseases, and may potentially be applied to other common and rare diseases due to the increasingly appreciated clinical significance of the complement system.^{22,47} Also, the therapeutic potential of CD14 inhibition has been demonstrated in various models of acute systemic inflammation, especially in combination with complement inhibition.⁴⁶

From this and a previous study, we know that IgG2/4 antibodies may induce a modest degree of complement activation, which can be measured as TCC formation in human and porcine blood, as well as pro-inflammatory cytokine release in porcine blood.¹² It appears that these effects are dependent on cell line-specific *N*-glycosylation of light and/or heavy chains, which is known to influence effector molecule binding in addition to antibody stability, pharmacokinetics, and pharmacodynamics.^{4,35} Both TCC and cytokine levels were largely reduced when NHDL and r18D11 were expressed by CHO cells instead of HEK293E cells. Also, CHO-produced NHDL did not bind human FcγRI, while HEK293E-produced NHDL was found to have some affinity. Notably, eculizumab is produced in murine NS0 cells, while upcoming eculizumab biosimilars are produced in CHO cells.⁴⁸

When IgG2/4 antibodies were expressed in CHO and HEK293E, the main difference in *N*-glycosylation of Asn297 in the C_H2 domain was the lower degree of terminal galactosylation of 4-*N*-acetylglucosamine-1-fucose-3-mannose (4GlcNac-1Fuc-3Man) in CHO compared to HEK293E cells. Non-galactosylated

4GlcNAc-1Fuc-3Man has also been shown to be common for other IgG subclasses expressed in CHO cells, *i.e.*, IgG1.⁴⁹ Higher degree of *N*-glycosylation, in particular the presence of terminal galactose moieties, may increase antibody complement-dependent cytotoxicity as well as FcγRIIIa-mediated ADCC.³⁶ Therefore, the lower degree of galactosidation when expressed from CHO compared to HEK293E cells may account for reduced induction of cytokine release and TCC formation by CHO-produced NHDL and r18D11.

Previously, we showed that HEK293E-produced IgG2/4 antibodies, including raNIP, did not bind human C1q and FcγRI, IIb, IIIa, and IIIb *in vitro*.¹² Importantly, CHO-produced IgG2/4 antibodies did not bind FcγRIIIa, which appears to be a major mediator of therapeutic antibody efficacy.³⁶ Both HEK293E- and CHO-produced IgG2/4 antibodies, however, had some affinity toward activating FcγRIIa, which may result in limited induction of effector functions.⁴⁹ Notably, FcγRIIa binding has been reported to be independent of the presence of terminal galactose,³⁶ which is in line with our study results. Nevertheless, glycoengineering of either the antibody or the expressing host cell line may be applied to render therapeutic IgG2/4 antibodies even more “effector-less”.^{49–51}

The residual effector functions of IgG2/4 antibodies need to be taken into account. However, when an anti-CD14 IgG2/4 antibody is combined with complement factor C3 or C5 inhibitory reagents, which we propose for treatment of certain acute inflammatory events,³³ the adverse effect on complement activation will most likely be suppressed by the inhibitors. NHDL will, in any case, provide a proper control antibody in both *in vitro* experiments and *in vivo* animal models, as long as the pharmacokinetics are similar. Future studies will reveal whether it also can be used as a placebo reagent in clinical studies.

Materials and methods

Blocking antibodies

The mouse/human chimeric IgG2/4 anti-human and porcine CD14 antibodies r18D11 and rMil2 were constructed and produced in our laboratory as previously reported.¹² The same applies to the hapten 4-hydroxy-3-iodo-5-nitrophenylacetic acid (NIP)-specific control antibody raNIP. Anti-human CD14 mouse antibody clone 18D11 was purchased from Diatec (Diatec Monoclonals AS, Oslo, Norway). The humanized IgG2/4 anti-human C5 antibody eculizumab (Soliris®) was obtained from Alexion Pharmaceuticals Inc. (Cheshire, CT, USA). For flow cytometry analyses, the rIgG2/4 antibodies NHDL, r18D11 and rMil2, as well as anti-human CD14 clone 18D11 and eculizumab were conjugated with PE using Lightning-Link® R-Phycoerythrin Conjugation Kit (Innova Biosciences, 703–0010). FITC-conjugated anti-porcine CD14 mouse antibody clone Mil2 and a FITC-conjugated mIgG2b control antibody were purchased from AbD Serotec (Bio-Rad AbD Serotec Ltd., MCA1218F).

Construction of plasmid DNA for expression of recombinant IgG2/4 antibody NHDL

Variable gene retrieval and cloning of constant regions of the recombinant mouse-human chimeric IgG2/4 antibodies were described in detail previously.^{12,42} Briefly, two plasmids containing oriP, pLNOH2 and pLNOK, were constructed for each recombinant antibody, encoding the heavy and the kappa light chain, respectively. The variable regions for the NHDL antibody were retrieved from monoclonal mouse antibodies raised against (1) a hapten (NIP) for the heavy chain, and (2) human CD14 (clone 18D11) for the light chain. Thus, the name NHDL stands for NIP heavy chain (NH) and 18D11 light chain (DL). The sequence for the human IgG2/4 hybrid constant region of the heavy chain was retrieved from the literature.¹³

Analytical scale NHDL expression and purification

Adherent HEK293-EBNA (HEK293E) cells were thawed and subcultured for two passages at 5% CO₂ and 37°C in DMEM containing 4.5 g/L L-glucose (Lonza, BE12–614F) and supplemented with 10% Fetal Bovine Serum Superior EU (Biochrom, Merck Millipore, BCHRS0615), 50 µg/mL G418 (Invitrogen, 10131–019), 4 mM L-glutamine (Lonza, BE17–605E), 10,000 U/mL penicillin, and 10,000 mg/mL streptomycin (Lonza, DE17–602E). Cells were transiently transfected with Lipofectamine 2000 (Invitrogen, 11668–019) according to the manufacturer’s protocol using a heavy chain-encoding plasmid (pLNOK) to light chain-encoding plasmid (pLNOH) ratio of 1:1. As a transient batch-batch procedure, cells were kept in serum-free OptiMEM (Invitrogen, 31985–047) for 12 days, and the antibody was harvested from the supernatant every third day. The supernatant was cleared from cell debris by centrifugation (5 min, 250 ×g) and vacuum filtration through 0.22 µm PES (TPP Techno Plastic Products AG, 99250) prior to antibody purification (see below). The antibody titer was estimated by standard ELISA using Goat Anti-Human Ig Fc pooled antisera (SouthernBiotech), either unconjugated as coat (2047–01) or horseradish peroxidase (HRP)-conjugated as capture (2047–05). The chromogenic readout was achieved by the addition of hydrogen peroxide as a substrate in ABTS buffer (Sigma-Aldrich, A9941–100TAB), and the signal was detected at 405 nm using an MRX plate reader from Dynex Technologies (Chantilly, VA). The antibody-containing cell culture supernatant was concentrated using Vivacell 100 PES concentrators with a 30K MWCO (Sartorius, VC1022). The antibody was purified using NAb Protein A Plus spin columns (Pierce Biotechnology, 89948) following the manufacturer’s instructions. Final buffer exchange to phosphate-buffered saline (PBS) pH7.4 and concentration to up to 1 mg/mL was done using concentrators with a 20K MWCO (Pierce Biotechnology, 87750).

SDS-PAGE, native PAGE, and western blot

The materials for PAGE were purchased from Bio-Rad (Bio-Rad Laboratories, Inc., Hercules, CA). The antibody preparation was monitored by standard non-denaturing SDS-PAGE

using Mini-PROTEAN Precast Gels (4–15%, 456–1084) and Tris-Glycine SDS buffer (161–0772). Antibody-antigen complexes were run on native PAGE using Mini-PROTEAN Precast Gels (4–15%) and Tris-Glycine buffer (161–0734). Gels were stained using Biosafe Coomassie G250 (161–0786).

For immunoblotting, proteins were transferred onto Protran NC membrane (0.45 μ m; Amersham, 10600003) and incubated with goat anti-human kappa light chain antibody (SouthernBiotech, 2060–01) prior to HRP-conjugated rabbit anti-goat IgG antibody (SouthernBiotech, 6160–05). ECL was performed with SuperSignal[®]West Dura Extended Duration substrate (Pierce, 34075) and detected using ChemiDoc XRS+ (Bio-Rad Laboratories, Inc., Hercules, CA).

***In vitro* complex formation with recombinant sCD14**

IgG2/4 antibodies were incubated 10 min at room temperature (RT) with recombinant soluble human CD14 (sCD14; ~50 kDa), either at molar excess of either molecule or at equimolar amounts, and run on native PAGE at 125 V for 90 min. Recombinant sCD14 was constructed as C-terminally octa-His-tagged protein, lacking the C-terminal eight amino acids (aa368–375) in order to avoid glycosylphosphatidylinositol anchoring, as described by Hailman *et al.*⁵² Soluble CD14 was expressed into cell culture medium of transiently transfected (Lipofectamine 2000) HEK293E cells, and purified using HisPur[™] Ni-NTA Spin Purification Kit (Pierce, 88228). Expression and purity of sCD14 were confirmed by SDS-PAGE and immunoblot using mouse anti-hexa His antibody (clone 13/45/31–2; Pierce, MA1-4806).

Size exclusion chromatography

Protein-A purified recombinant IgG2/4 antibodies were fractionated by SEC using a Superdex 200 10/300 column (GE Healthcare, 28-9909-44) connected to an ÄKTA-FPLC instrument (GE Healthcare, Buckinghamshire, UK). Fractions containing monomeric recombinant IgG2/4 variants were up-concentrated using Amicon[®] Ultra centrifugal filters (Millipore, UFC205024).

Differential scanning fluorimetry

DSF was performed using a LightCycler[®] 480 RT-PCR instrument (Roche Diagnostics Norge AS, Oslo, Norway). Sypro[®] Orange (Sigma-Aldrich, S5692) was mixed (1:1000) with purified antibody (0.1 mg/mL) in 25 μ L PBS. Samples were run in triplicates in LightCycler[®] 480 multi-well plates 96 (Roche, 04729692001). The RT-PCR instrument was programmed to ramp the temperature from 20°C to 95°C within 30 min, after an initial period of 10 min at 20°C. Data were collected every 0.5°C using 450 nm excitation and 568 nm emission filters. Data transformation and analysis were performed using the DSF analysis protocol as described by Niesen *et al.*⁵³ To calculate the T_m values, the lowest temperature value at steady state (before protein starts to unfold) and the temperature value at highest fluorescence intensity (protein is completely unfolded) were used.

Whole blood model of inflammation according to Mollnes et al.³²

Fresh human or porcine whole blood from three independent individuals was anti-coagulated with 50 μ g/mL lepirudin (Refludan[®], Pharmion, Copenhagen, Denmark) and incubated in 1.8 mL Cryo Tube vials (Nunc, 377267) for 120 min at 37°C on a rock'n'roller with either sterile PBS with MgCl₂ and CaCl₂ (Sigma-Aldrich, D8662) or an inflammation-inducing agent. Here, we used 100 ng/mL ultrapure LPS from *E. coli* O111:B4 (InvivoGen, tlr1-3pelps) for human blood and 1x10⁵/mL heat-inactivated *E. coli* strain LE392 (ATCC 33572) for porcine blood. The incubation was further done in the presence or absence of increasing or fixed amounts of the IgG2/4 control antibody NHDL, raNIP, anti-human CD14 (r18D11), and anti-porcine CD14 (rMil2). To stop the response, 10 mM (human blood) or 20 mM (porcine blood) EDTA was added, and plasma was gained by 15 min centrifugation at 3220 xg and 4°C.

Enzyme immunoassays

Human and porcine plasma cytokines were quantified using Luminex technology using Bio-Plex[®] Multiplex Immunoassays from Bio-Rad and ProcartaPlex[™] Multiplex Immunoassays from eBioscience, respectively. Complement activation in porcine samples was measured as soluble terminal C5b-9 complement complex (sC5b-9, TCC) generation using standard ELISA and complement arbitrary units (CAU)/mL as readout.⁵⁴ Briefly, ascites containing monoclonal anti-human C9 neoepitope antibody, clone aE11,⁵⁵ was used for capture and biotinylated (EZ-Link[®] NHS-SS-Biotin; Pierce, 21331) anti-human C6 (Quidel, A219) for detection. Further incubations with streptavidin-coupled peroxidase (GE Healthcare, RPN1231) and H₂O₂ in ABTS buffer generated a specific signal, which was recorded at 405 nm using an MRX plate reader from Dynex Technologies. Antibody titers of IgG2/4 were revealed by standard sandwich ELISA using polyclonal goat anti-human IgG Fc antibody (Southern Biotech) for capture (unconjugated, 2047–01) as well as for detection (HRP-conjugated, 2047–05).

Immunoprecipitation for mass spectrometry

Purified IgG2/4 antibodies (100 μ g NHDL, r18D11, and rMil2) and commercial anti-C5 eculizumab (100 μ g) were coupled to 10 mg magnetic beads using Dynabeads[™] Antibody Coupling Kit (Novex[™], LifeTechnologies, 143-11D). Coupling efficiency was 85–99%, according to unbound IgG estimated by ELISA. Plasma pools were generated from fresh human (n = 6) or porcine (n = 9) blood, anti-coagulated with 50 μ g/mL lepirudin (Refludan[®]), by centrifugation at 3000 xg for 20 min or 10 min, respectively. For immunoprecipitation, plasma was diluted in 4x Vol Pierce[™] IP lysis buffer (87787) containing Pierce[™] Protease and Phosphatase Inhibitor Mini Tablets (88668). Further, 10 μ g bead-coupled IgG were incubated with 500 μ L diluted human or porcine plasma pools rotating overnight at 4°C. To control for technical artifacts and putative nonspecific or intrinsic binding of murine IgG to human and porcine plasma proteins, immunoprecipitation using a commercial magnetic bead-coupled anti-human CD3 mouse IgG1 antibody (Dynabeads[®] CD3, Dynal Biotech

ASA) was performed in parallel. The putative antibody-antigen complexes were washed twice on a magnetic stand with 0.5 mL IP lysis buffer and eluted with 50 μ L Laemmli buffer containing 5% β -mercaptoethanol by boiling 5 min at 95°C. Of the latter, 10 μ L was briefly separated by SDS-PAGE, before the gel was Coomassie stained and the stained broad bands were cut for downstream mass spectrometry sample preparation.

Mass spectrometry and data processing

Gel pieces were subjected to in-gel reduction, alkylation, and tryptic digestion using 6 ng/ μ L trypsin (Promega, V511A). OMIX C18 tips (Varian, Inc., A57003100k) were used for sample clean-up and concentration. Peptide mixtures containing 0.1% formic acid were loaded onto an EASY-nLC1000 system (Thermo Fisher Scientific, Waltham, MA) and EASY-Spray column (C18, 2 μ m, 100 Å , 50 μ m, 50 cm; Thermo Fisher Scientific, ES803). Peptides were fractionated using a 2 – 100% acetonitrile gradient in 0.1% formic acid over 50 min at a flow rate of 200 nL/min. The separated peptides were analyzed using a Q-Exactive mass spectrometer (Thermo Fisher Scientific). Data were collected in data-dependent mode using a Top10 method. The raw data were processed using the Proteome Discoverer 2.0 software (Thermo Scientific). The fragmentation spectra were searched against the Swissprot_2015_05 database using an in-house Mascot server (Matrix Sciences, UK). Peptide mass tolerances used in the search were 10 ppm, and fragment mass tolerance was 0.02 Da. Peptide ions were filtered using a false discovery rate (FDR) set to 1% for peptide identifications.

For hierarchical clustering, raw data were processed by the MaxQuant software v 1.5.0.15 with the integrated Andromeda search engine using the label-free quantification (LFQ) method. MS/MS data were searched against the Uniprot human and porcine databases from 2015. An FDR ratio of 0.01 was needed to give a protein identification. Hierarchical clustering was done with log₂ transformed LFQ intensities using average Euclidian distance.

Flow cytometry analyses

For competitive assays, fresh human or porcine lepirudin anti-coagulated blood (100 μ L per test) was pre-incubated 15 min at RT with increasing amounts of unconjugated IgG2/4 control antibody NHDL and unconjugated anti-human CD14 (clone r18D11) or anti-porcine CD14 (clone rMil2) antibodies, respectively. Afterward, the blood was incubated for an additional 15 min at RT with PE-conjugated anti-human CD14 (clone 18D11, 15 μ g/mL) or FITC-conjugated anti-porcine CD14 (clone Mil2, 100 μ g/mL) antibody. A FITC-conjugated mIgG2b control antibody was included to control for background fluorescence in porcine samples.

For direct binding assays, fresh human or porcine lepirudin anti-coagulated blood (100 μ L per test) was incubated with increasing amounts of R-PE-conjugated NHDL for 15 min at RT. The results were compared to binding of R-PE-conjugated anti-human CD14 (r18D11; 10 ng/mL to 10 μ g/mL) or anti-porcine CD14 (rMil2; 10 and 50 μ g/mL) antibodies. As controls in human blood, four blood samples were pre-incubated with

15 μ g/mL unconjugated NHDL or r18D11 prior to the addition of 10 μ g/mL PE-conjugated antibody. As negative control in porcine blood, one blood sample was incubated with the irrelevant PE-conjugated anti-human CD14 antibody (r18D11).

Subsequently, red blood cells were lysed and remaining blood cells were fixed using Lyse/Fix solution (BD Biosciences, 558049) prior to analyses on an LSRII flow cytometer (BD Biosciences, Franklin Lakes, NJ, USA) using FACS Diva 7 software. Human monocyte and porcine granulocyte populations were selected based on the forward scatter/side scatter dot plot, and antibody binding was recorded as mean fluorescence intensity (MFI).

Complement C5 binding and activation in human serum

For C5 binding analyses, 156 μ L of a human serum pool was incubated for 30 min at 37°C with 40 μ L rIgG2/4 isotype control antibody NHDL or anti-C5 IgG2/4 antibody eculizumab at final concentrations of 1.5 μ g/mL to 50 μ g/mL. C5 binding was quantified using a recently established enzyme-immunoassay for the detection of eculizumab-C5 complexes,³⁴ using an anti-C5 antibody as capture and an HRP-conjugated anti-human IgG4 antibody for detection.

For C5 blocking analyses, 156 μ L of a human serum pool was incubated for 30 min at 37°C with 40 μ L PBS, NHDL or eculizumab (200 μ g/mL final concentration), and 4 μ L PBS or heat-aggregated IgG (HAIGG; 1 mg/mL final concentration). Complement activation was measured as TCC generation in CAU/mL as described above for *Enzyme immunoassays*.

Production scale expression and two-step purification of rIgG2/4 antibodies

CHO-K1SP cell pools stably expressing NHDL or r18D11 were generated by Genscript Inc. (Piscataway, NJ, USA). The suspension culture was kept at 37°C, 5% CO₂, >90% relative humidity and 120 rpm using a Kuehner LT-X shaking incubator (Adolf Kühner AG, Birsfelden, Switzerland) at 50 mm rotating diameter. Freshly thawed cells were resuspended at 4 \times 10⁵/mL in CD CHO medium (Gibco™, Life Technologies, 10743–011) containing L-Methionine sulfoximine (Merck Millipore, GSS-1015-F) and anti-clumping agent (Gibco™, Life Technologies, 01-0057DG), and cultivated for three passages using sterile 125 mL Erlenmeyer flasks (EF) (Corning, CLS431143-50EA). For fed-batch production culture, 4 \times 10⁷ cells in 100 mL CD FortiCHO medium (Invitrogen™, Life Technologies, A11483-01) containing L-methionine sulfoximine and anti-clumping agent were cultivated in 500 mL EF (Corning, CLS431145-25EA) for a period of 14 days. CHO CD EfficientFeed™ B Liquid Nutrient Supplement (Invitrogen™, Life Technologies, A10240-01) was added at 10% (v/v) every second day for 8 days, before continuation for another 6 days without feed. On day 14, cell viability was still above 50% and cell culture supernatant was harvested by centrifugation and filtration (0.22 μ m PES; TPP). The protocol can be scaled up using one or more 1000 mL EF (Corning, CLS431147-25EA) or TubeSpin® Bioreactor 600 (TPP, 87600) and 200 mL to 320 mL expression medium \pm feed per flask. The antibody was purified on an NGC Quest 10 (Bio-Rad Laboratories, Inc.,

Hercules, CA) in two steps: 1) Protein-A affinity chromatography using Foresight UNOsphere SUPRA (Bio-Rad, 732–4749), and 2) preparative SEC using HiPrep 26/60 Sephacryl S-300HR (GE Healthcare, 17-1196-01). Fractions containing monomeric recombinant IgG2/4 antibody were up-concentrated using Amicon® Ultra centrifugal filters (Millipore, UFC205024) or Vivacell® 100 PES centrifugal concentrators (Sartorius, VC1022) and stored at –80°C.

FcγR binding by ELISA

ELISA 96-well plates were coated with 100 mL of titrated amounts (10,000.0–4.6 ng/mL) of HEK293E- or CHO-produced NHDL or r18D11 in PBS (Sigma-Aldrich, D8537-500ML) and incubated overnight at 4°C. After washing, 1 µg/ml GST-tagged hFcγRI, hFcγRIIa, and FcγRIIIa in 4% skim milk (PanReac AppliChem, 0830,5000) in PBS containing 0.05% Tween20 (Sigma-Aldrich, P1379_500ML) (PBST) were incubated for 1 h at RT before being washed as above. Bound receptors were detected using an HRP-conjugated goat anti-GST Ab (Rockland Immunochemicals Inc., 600-103-200) diluted 1:8000 in 4% skim milk/PBST. After washing, 100 µL TMB substrate (Millipore, CL07-1000ML) was added to each well, and reactions were stopped by adding 100 µL 1 M HCl. The absorbance was measured at 450 nm using a Sunrise spectrophotometer (Tecan Trading AG, Switzerland).

Animals

Porcine blood samples were drawn from healthy Norwegian landrace piglets (*Sus scrofa domesticus*), prior to their use in independent *in vivo* studies.

Abbreviations

CAU	complement arbitrary units
CD14	cluster of differentiation 14
C _H	constant heavy chain
CHO	Chinese ovary hamster
DSF	differential scanning fluorimetry
<i>E. coli</i>	<i>Escherichia coli</i>
ELISA	enzyme-linked immunosorbent assay
FcγR	Fc gamma receptor
LC-MS	liquid chromatography – mass spectrometry
MFI	mean fluorescence intensity
NIP	4-hydroxy-3-iodo-5-nitrophenylacetic acid
PSM	peptide spectrum matches
S.D.	standard deviation
S.E.M.	standard error of the mean
SEC	size exclusion chromatography
TLR	Toll-like receptor
T _m	melting temperature
V _H	variable heavy chain
V _L	variable light chain

Acknowledgments

This work was supported by the Northern Norway Regional Health Authority under Grant 8416/SFP1083-13, The Norwegian Council of Cardiovascular Disease (NCCD-2014) and the Odd Fellow Foundation (OFF-2015). J.T.A. was in part supported by the Research Council of Norway through its Centers of Excellence funding scheme (grant no.

179573), the Research Council of Norway (grant no. 287927), and the South-Eastern Norway Regional Health Authority (grant no. 2018052).

Disclosure of potential conflicts of interest

No potential conflict of interest was reported by the authors.

Ethics

The study was approved by the Norwegian Government Regional Committee for Medical Research and by the Norwegian Animal Research Authority. Informed written consent was given in advance by all healthy human blood donors.

Funding

This work was supported by Helse Sør-Øst RHF [2018052]; [Norges Forskningsråd [287927]; Norges Forskningsråd [179573]; Norwegian council of cardiovascular disease [NCCD-2014]; Helse Nord RHF [8416/SFP1083-13]; Odd Fellow Foundation [OFF-2015].

ORCID

Corinna Lau  <http://orcid.org/0000-0003-1750-8065>
 Martin Berner McAdam  <http://orcid.org/0000-0001-9385-6964>
 Jack Ansgar Bruun  <http://orcid.org/0000-0003-0614-2790>
 Hilde Fure  <http://orcid.org/0000-0002-3634-0969>
 Terje Espevik  <http://orcid.org/0000-0003-0354-5068>
 Anders Moen  <http://orcid.org/0000-0002-6936-0747>
 Jan Terje Andersen  <http://orcid.org/0000-0003-1710-1628>
 Tom Eirik Mollnes  <http://orcid.org/0000-0002-5785-802X>

References

- Carter PJ, Lazar GA. Next generation antibody drugs: pursuit of the 'high-hanging fruit'. *Nat Rev Drug Discov.* 2018;17:197–223. doi:10.1038/nrd.2017.227.
- Vidarsson G, Dekkers G, Rispens T. IgG subclasses and allotypes: from structure to effector functions. *Front Immunol.* 2014;5:520. doi:10.3389/fimmu.2014.00520.
- Stapleton NM, Andersen JT, Stermerding AM, Bjarnarson SP, Verheul RC, Gerritsen J, Zhao Y, Kleijer M, Sandlie I, de Haas M, et al. Competition for FcRn-mediated transport gives rise to short half-life of human IgG3 and offers therapeutic potential. *Nat Commun.* 2011;2:599. doi:10.1038/ncomms1608.
- Liu L. Antibody glycosylation and its impact on the pharmacokinetics and pharmacodynamics of monoclonal antibodies and Fc-fusion proteins. *J Pharm Sci.* 2015;104:1866–84. doi:10.1002/jps.24444.
- Mimura Y, Katoh T, Saldova R, O'Flaherty R, Izumi T, Mimura-Kimura Y, Utsunomiya T, Mizukami Y, Yamamoto K, Matsumoto T, et al. Glycosylation engineering of therapeutic IgG antibodies: challenges for the safety, functionality and efficacy. *Protein Cell.* 2018;9:47–62. doi:10.1007/s13238-017-0433-3.
- Schlothauer T, Herter S, Koller CF, Grau-Richards S, Steinhart V, Spick C, Kubbies M, Klein C, Umama P, Mossner E. Novel human IgG1 and IgG4 Fc-engineered antibodies with completely abolished immune effector functions. *Protein Eng Des Sel.* 2016;29:457–66. doi:10.1093/protein/gzw040.
- Wang X, Mathieu M, Brezski RJ. IgG Fc engineering to modulate antibody effector functions. *Protein Cell.* 2018;9:63–73. doi:10.1007/s13238-017-0473-8.
- Saunders KO. Conceptual approaches to modulating antibody effector functions and circulation half-life. *Front Immunol.* 2019;10:1296. doi:10.3389/fimmu.2019.01296.

9. An Z, Forrest G, Moore R, Cukan M, Haytko P, Huang L, Vitelli S, Zhao JZ, Lu P, Hua J, et al. IgG2m4, an engineered antibody isotype with reduced Fc function. *MAbs*. 2009;1:572–79. doi:10.4161/mabs.1.6.10185.
10. Vafa O, Gilliland GL, Brezski RJ, Strake B, Wilkinson T, Lacy ER, Scallion B, Teplyakov A, Malia TJ, Strohl WR. An engineered Fc variant of an IgG eliminates all immune effector functions via structural perturbations. *Methods*. 2014;65:114–26. doi:10.1016/j.ymeth.2013.06.035.
11. Bruhns P, Iannascoli B, England P, Mancardi DA, Fernandez N, Jorieux S, Daeron M. Specificity and affinity of human Fcgamma receptors and their polymorphic variants for human IgG subclasses. *Blood*. 2009;113:3716–25. doi:10.1182/blood-2008-09-179754.
12. Lau C, Gunnarsen KS, Hoydahl LS, Andersen JT, Berntzen G, Pharo A, Lindstad JK, Ludviksen JK, Brekke OL, Barratt-Due A, et al. Chimeric anti-CD14 IGG2/4 Hybrid antibodies for therapeutic intervention in pig and human models of inflammation. *J Immunol*. 2013;191:4769–77. doi:10.4049/jimmunol.1301653.
13. Mueller JP, Giannoni MA, Hartman SL, Elliott EA, Squinto SP, Matis LA, Evans MJ. Humanized porcine VCAM-specific monoclonal antibodies with chimeric IgG2/G4 constant regions block human leukocyte binding to porcine endothelial cells. *Mol Immunol*. 1997;34:441–52. doi:10.1016/S0161-5890(97)00042-4.
14. Rother RP, Rollins SA, Mojcik CF, Brodsky RA, Bell L. Discovery and development of the complement inhibitor eculizumab for the treatment of paroxysmal nocturnal hemoglobinuria. *Nat Biotechnol*. 2007;25:1256–64. doi:10.1038/nbt1344.
15. Wong EK, Kavanagh D. Anticomplement C5 therapy with eculizumab for the treatment of paroxysmal nocturnal hemoglobinuria and atypical hemolytic uremic syndrome. *Transl Res*. 2015;165:306–20. doi:10.1016/j.trsl.2014.10.010.
16. Dmytrijuk A, Robie-Suh K, Cohen MH, Rieves D, Weiss K, Pazdur R. FDA report: eculizumab (Soliris) for the treatment of patients with paroxysmal nocturnal hemoglobinuria. *Oncologist*. 2008;13:993–1000. doi:10.1634/theoncologist.2008-0086.
17. Merle NS, Noe R, Halbwachs-Mecarelli L, Fremeaux-Bacchi V, Roumenina LT. Complement system part II: role in immunity. *Front Immunol*. 2015;6:257. doi:10.3389/fimmu.2015.00257.
18. Ricklin D, Hajishengallis G, Yang K, Lambris JD. Complement: a key system for immune surveillance and homeostasis. *Nat Immunol*. 2010;11:785–97. doi:10.1038/ni.1923.
19. Ricklin D, Lambris JD. Complement in immune and inflammatory disorders: pathophysiological mechanisms. *J Immunol*. 2013;190:3831–38. doi:10.4049/jimmunol.1203487.
20. Melis JP, Strumane K, Ruuls SR, Beurskens FJ, Schuurman J, Parren PW. Complement in therapy and disease: regulating the complement system with antibody-based therapeutics. *Mol Immunol*. 2015;67:117–30. doi:10.1016/j.molimm.2015.01.028.
21. Morgan BP, Harris CL. Complement, a target for therapy in inflammatory and degenerative diseases. *Nat Rev Drug Discov*. 2015;14:857–77. doi:10.1038/nrd4657.
22. Ricklin D, Barratt-Due A, Mollnes TE. Complement in clinical medicine: clinical trials, case reports and therapy monitoring. *Mol Immunol*. 2017;89:10–21. doi:10.1016/j.molimm.2017.05.013.
23. Woodruff TM, Nandakumar KS, Tedesco F. Inhibiting the C5-C5a receptor axis. *Mol Immunol*. 2011;48:1631–42. doi:10.1016/j.molimm.2011.04.014.
24. Egge KH, Barratt-Due A, Nymo S, Lindstad JK, Pharo A, Lau C, Espevik T, Thorgersen EB, Mollnes TE. The anti-inflammatory effect of combined complement and CD14 inhibition is preserved during escalating bacterial load. *Clin Exp Immunol*. 2015;181:457–67. doi:10.1111/cei.12645.
25. Skjeflo EW, Sagatun C, Dybwik K, Aam S, Urving SH, Nunn MA, Fure H, Lau C, Brekke OL, Huber-Lang M, et al. Combined inhibition of complement and CD14 improved outcome in porcine polymicrobial sepsis. *Crit Care*. 2015;19:415. doi:10.1186/s13054-015-1129-9.
26. Baumann CL, Aspalter IM, Sharif O, Pichlmair A, Bluml S, Grebien F, Bruckner M, Pasierbek P, Aumayr K, Planyavsky M, et al. CD14 is a coreceptor of Toll-like receptors 7 and 9. *J Exp Med*. 2010;207:2689–701. doi:10.1084/jem.20101111.
27. Osterbye T, Funda DP, Fundova P, Mansson JE, Tlaskalova-Hogenova H, Buschard K. A subset of human pancreatic beta cells express functional CD14 receptors: a signaling pathway for beta cell-related glycolipids, sulfatide and beta-galactosylceramide. *Diabetes Metab Res Rev*. 2010;26:656–67. doi:10.1002/dmrr.1134.
28. Pugin J, Heumann ID, Tomasz A, Kravchenko VV, Akamatsu Y, Nishijima M, Glauser MP, Tobias PS, Ulevitch RJ. CD14 is a pattern recognition receptor. *Immunity*. 1994;1:509–16. doi:10.1016/1074-7613(94)90093-0.
29. Weber C, Muller C, Podszuweit A, Montino C, Vollmer J, Forsbach A. Toll-like receptor (TLR) 3 immune modulation by unformulated small interfering RNA or DNA and the role of CD14 (in TLR-mediated effects). *Immunology*. 2012;136:64–77. doi:10.1111/j.1365-2567.2012.03559.x.
30. Chenevier-Gobeaux C, Borderie D, Weiss N, Mallet-Coste T, Claessens YE. Presepsin (sCD14-ST), an innate immune response marker in sepsis. *Clin Chim Acta*. 2015;450:97–103. doi:10.1016/j.cca.2015.06.026.
31. Huber-Lang M, Barratt-Due A, Pischke SE, Sandanger O, Nilsson PH, Nunn MA, Denk S, Gaus W, Espevik T, Mollnes TE. Double blockade of CD14 and complement C5 abolishes the cytokine storm and improves morbidity and survival in polymicrobial sepsis in mice. *J Immunol*. 2014;192:5324–31. doi:10.4049/jimmunol.1400341.
32. Mollnes TE, Brekke OL, Fung M, Fure H, Christiansen D, Bergseth G, Videm V, Lappgard KT, Kohl J, Lambris JD. Essential role of the C5a receptor in E coli-induced oxidative burst and phagocytosis revealed by a novel lepirudin-based human whole blood model of inflammation. *Blood*. 2002;100:1869–77.
33. Barratt-Due A, Pischke SE, Brekke OL, Thorgersen EB, Nielsen EW, Espevik T, Huber-Lang M, Mollnes TE. Bride and groom in systemic inflammation—the bells ring for complement and Toll in cooperation. *Immunobiology*. 2012;217:1047–56. doi:10.1016/j.imbio.2012.07.019.
34. Hallstensen RF, Bergseth G, Foss S, Jaeger S, Gedde-Dahl T, Holt J, Christiansen D, Lau C, Brekke OL, Armstrong E, et al. Eculizumab treatment during pregnancy does not affect the complement system activity of the newborn. *Immunobiology*. 2015;220:452–59. doi:10.1016/j.imbio.2014.11.003.
35. Schroeder HW Jr., Cavacini L. Structure and function of immunoglobulins. *J Allergy Clin Immunol*. 2010;125:S41–52. doi:10.1016/j.jaci.2009.09.046.
36. Abes R, Teillaud JL. Impact of glycosylation on effector functions of therapeutic IgG. *Pharmaceuticals (Basel)*. 2010;3:146–57. doi:10.3390/ph3010146.
37. Hamel PA, Klein MH, Dorrington KJ. The role of the VL- and VH-segments in the preferential reassociation of immunoglobulin subunits. *Mol Immunol*. 1986;23:503–10. doi:10.1016/0161-5890(86)90113-6.
38. Hamel PA, Klein MH, Smith-Gill SJ, Dorrington KJ. Relative noncovalent association constant between immunoglobulin H and L chains is unrelated to their expression or antigen-binding activity. *J Immunol*. 1987;139:3012–20.
39. Hasegawa H. Aggregates, crystals, gels, and amyloids: intracellular and extracellular phenotypes at the crossroads of immunoglobulin physicochemical property and cell physiology. *Int J Cell Biol*. 2013;2013:604867. doi:10.1155/2013/604867.
40. Stoops J, Byrd S, Hasegawa H. Russell body inducing threshold depends on the variable domain sequences of individual human IgG clones and the cellular protein homeostasis. *Biochim Biophys Acta*. 2012;1823:1643–57. doi:10.1016/j.bbamer.2012.06.015.
41. Berntzen G, Lunde E, Flobakk M, Andersen JT, Lauvrak V, Sandlie I. Prolonged and increased expression of soluble Fc receptors, IgG and a TCR-Ig fusion protein by transiently transfected adherent 293E cells. *J Immunol Methods*. 2005;298:93–104. doi:10.1016/j.jim.2005.01.002.

42. Norderhaug L, Olafsen T, Michaelsen TE, Sandlie I. Versatile vectors for transient and stable expression of recombinant antibody molecules in mammalian cells. *J Immunol Methods*. 1997;204:77–87. doi:10.1016/S0022-1759(97)00034-3.
43. Sela-Culang I, Kunik V, Ofran Y. The structural basis of antibody-antigen recognition. *Front Immunol*. 2013;4:302. doi:10.3389/fimmu.2013.00302.
44. Strohl WR. Current progress in innovative engineered antibodies. *Protein Cell*. 2018;9:86–120. doi:10.1007/s13238-017-0457-8.
45. Kamath AV. Translational pharmacokinetics and pharmacodynamics of monoclonal antibodies. *Drug Discov Today Technol*. 2016;21–22:75–83. doi:10.1016/j.ddtec.2016.09.004.
46. Barratt-Due A, Pischke SE, Nilsson PH, Espevik T, Mollnes TE. Dual inhibition of complement and Toll-like receptors as a novel approach to treat inflammatory diseases-C3 or C5 emerge together with CD14 as promising targets. *J Leukoc Biol*. 2017;101:193–204. doi:10.1189/jlb.3VMR0316-132R.
47. Ricklin D, Mastellos DC, Reis ES, Lambris JD. The renaissance of complement therapeutics. *Nat Rev Nephrol*. 2018;14:26–47. doi:10.1038/nrneph.2017.156.
48. Generics and Biosimilars Initiative. Epirus expands biosimilars pipeline with bioceros acquisition. Pro pharma communications international. October 2, 2015 online post. <http://gabionline.net/layout/set/print/Pharma-News/Epirus-expands-biosimilars-pipeline-with-Bioceros-acquisition>.
49. Zheng K, Yarmarkovich M, Bantog C, Bayer R, Patapoff TW. Influence of glycosylation pattern on the molecular properties of monoclonal antibodies. *MAbs*. 2014;6:649–58. doi:10.4161/mabs.28588.
50. Li W, Zhu Z, Chen W, Feng Y, Dimitrov DS. Crystallizable fragment glycoengineering for therapeutic antibodies development. *Front Immunol*. 2017;8:1554. doi:10.3389/fimmu.2017.01554.
51. Wang Q, Chung CY, Chough S, Betenbaugh MJ. Antibody glycoengineering strategies in mammalian cells. *Biotechnol Bioeng*. 2018;115:1378–93. doi:10.1002/bit.26567.
52. Hailman E, Lichenstein HS, Wurfel MM, Miller DS, Johnson DA, Kelley M, Busse LA, Zukowski MM, Wright SD. Lipopolysaccharide (LPS)-binding protein accelerates the binding of LPS to CD14. *J Exp Med*. 1994;179:269–77. doi:10.1084/jem.179.1.269.
53. Niesen FH, Berglund H, Vedadi M. The use of differential scanning fluorimetry to detect ligand interactions that promote protein stability. *Nat Protoc*. 2007;2:2212–21. doi:10.1038/nprot.2007.321.
54. Bergseth G, Ludviksen JK, Kirschfink M, Giclas PC, Nilsson B, Mollnes TE. An international serum standard for application in assays to detect human complement activation products. *Mol Immunol*. 2013;56:232–39. doi:10.1016/j.molimm.2013.05.221.
55. Mollnes TE, Lea T, Harboe M, Tschopp J. Monoclonal antibodies recognizing a neoantigen of poly(C9) detect the human terminal complement complex in tissue and plasma. *Scand J Immunol*. 1985;22:183–95. doi:10.1111/sji.1985.22.issue-2.